

HIGH ORDER FAST ALGORITHM FOR THE CAPUTO FRACTIONAL DERIVATIVE*

KUN WANG[†] AND JIZU HUANG[‡]

Abstract. In the paper, we present a high order fast algorithm with almost optimum memory for the Caputo fractional derivative, which can be expressed as a convolution of $u'(t)$ with the kernel $(t_n - t)^{-\alpha}$. In the fast algorithm, the interval $[0, t_{n-1}]$ is split into nonuniform subintervals. The number of the subintervals is in the order of $\log n$ at the n -th time step. The fractional kernel function is approximated by a polynomial function of K -th degree with a uniform absolute error on each subinterval. We save $K + 1$ integrals on each subinterval, which can be written as a convolution of $u'(t)$ with a polynomial base function. As compared with the direct method, the proposed fast algorithm reduces the storage requirement and computational cost from $O(n)$ to $O((K + 1) \log n)$ at the n -th time step. We prove that the convergence rate of the fast algorithm is the same as the direct method even a high order direct method is considered. The convergence rate and efficiency of the fast algorithm are illustrated via several numerical examples.

Key words. Caputo fractional derivative, fast algorithm, polynomial approximation, error estimates, fractional diffusion equations.

AMS Subject Classifications: 65F10, 78M05

1. Introduction. In recent years, the fractional differential equation becomes popular since they can faithfully capture the dynamics of physical process in many scientific phenomena, such as the dynamics of biology, ecology, and control system [11, 12, 13, 14, 17, 18, 25, 27, 28, 29]. There are mainly two kinds of definitions of the fractional time derivative in the literatures: the Riemann–Liouville fractional derivative [3, 4] and the Caputo fractional derivative [11, 29, 32, 33, 36]. In fractional partial differential equations (PDEs), the time fractional derivatives are commonly defined using the Caputo fractional derivatives since the Riemann–Liouville approach needs initial conditions containing the limit values of Riemann–Liouville fractional derivative at the origin of time $t = 0$, whose physical meanings are not very clear. In the paper, we focus on the high order fast method of the PDEs including the Caputo fractional derivative which is defined by

$${}_0^C \mathcal{D}_t^\alpha u(t) = \frac{1}{\Gamma(1 - \alpha)} \int_0^t \frac{u'(x, \tau)}{(t - \tau)^\alpha} d\tau, \quad 0 < \alpha < 1, \quad (1.1)$$

where $\Gamma(\cdot)$ is the gamma function and t is in $[0, T]$.

One of the popular schemes of discretizing the Caputo fractional derivative is usually called $L1$ formula [9, 19, 32], which applies the piecewise linear interpolation of $u(x, t)$ with respect to t in the integrand on each subinterval. For $0 < \alpha < 1$, the scheme enjoys a $2 - \alpha$ order of convergence rate. Some other methods with a $2 - \alpha$ order of convergence rate are also studied, such as the Crank–Nicolson-Type discretization [36] and the matrix transfer technique [33]. By applying the fractional

* This work is supported by the National Natural Science Foundation of China (grants # 11501554, 91630205), and the Fundamental Research Funds for the Central Universities (project # 106112017CDJXY100006).

[†]College of Mathematics and Statistics, Chongqing University, Chongqing, 401331, China (kunwang@cqu.edu.cn).

[‡]LSEC, Institute of Computational Mathematics and Scientific/Engineering Computing, Academy of Mathematics and Systems Science, Chinese Academy of Sciences, Beijing(100190), China (huangjz@lsec.cc.ac.cn). Corresponding author: huangjz@lsec.cc.ac.cn.

linear multistep methods in discretizing the Caputo fractional derivative, an exactly second order scheme with unconditional stability is constructed in [34]. By using the piecewise quadratic interpolation of $u(t)$ in the integrand for the Caputo fractional derivative, Gao and Sun [8] propose a new discrete formula (called $L1 - 2$ formula) which achieves $3 - \alpha$ order accuracy. Recently, based on the block-by-block approach, Cao et al. improve the discretization in time and a scheme with order $3 + \alpha$ is successfully constructed in [2]. On the other hand, a scheme with spectral accuracy is also investigated in [17]. These direct methods require the storage of all previous solutions, which leads to $O(n)$ storage and $O(n)$ flops at the n -th time step. Therefore, an efficient and reliable fast method is needed for long time large scale simulation of fractional PDEs.

In order to save memory and computational cost, some fast methods are developed. In [21], a fast convolution method for the Caputo fractional derivative is proposed, in which the kernel function is first expressed by its inverse Laplace transform. The idea is then extended to calculate the Caputo fractional derivative in [20, 30, 35]. The storage requirement and the computational cost of those fast methods both are $O(\log n)$ at the n -th time step, which are less than that of the direct methods. In [29], the Laplace transform method is used to transform the fractional differential equation into an approximation local problem. In [16], the Gauss–Legendre quadrature is applied to construct a fast algorithm based on the formula $t^{\alpha-1} = \frac{1}{\Gamma(\alpha)\Gamma(1-\alpha)} \int_0^\infty e^{-\xi t} \xi^{-\alpha} d\xi$. The fast method is improved by Jiang et al. [11] by using the Gauss–Jacobi and Gauss–Legendre quadratures together, which only requires the storage and the computational cost in the order of $O(\log n)$ at the n -th time step. The fast scheme is proved to be unconditionally stable and has a convergence order of $2 - \alpha$ [11]. In [23], McLean proposes a fast method to approximate the fractional integral by replacing the fractional kernel with a degenerate kernel. In [1], a kernel compression method is presented to discretize the fractional integral operator, which is based on multipole approximation to the Laplace transform of the fractional kernel.

In this paper, we aim to present a high order fast algorithm with almost optimum memory for the Caputo fractional derivative, which has the same order of convergence rate as that of a given direct method. At each time step, the fractional derivative is decomposed into the local part and the history part. The local part, which is an integral on interval $[t_{n-1}, t_n]$, is calculated by a direct method. In order to evaluate the history part by a high efficient approach with low cost, we split the interval $[0, t_{n-1}]$ into nonuniform subintervals at the n -th time step. The total number of the subintervals is in the order of $\log n$. We save $K + 1$ integrals on each subinterval and evaluate the history part with those integrals. To reuse the storages in the previous time step, we approximate the fractional kernel function by a polynomial function with a uniform absolute error on the subintervals. As compared with a direct method based on a given polynomial interpolation of $u(t)$, the new proposed fast method is proved to enjoy the same convergence order by controlling the absolute error of the approximate polynomial function, but only requires computational storage and flops in the order of $\log n$ at the n -th time step.

The remainder of the paper is organized as follows. In Section 2, we describe the high order fast algorithm for the evolution of the Caputo fractional derivative and provide error analysis of our method. In Sections 3 and 4, we apply the proposed high order fast algorithm to solve the linear and nonlinear fractional diffusion PDEs. The stability and numerical error analysis for the new algorithm and some existing

methods are carefully studied. The numerical results demonstrate that our high order algorithm has the same convergence order as the corresponding direct method. Finally, some brief conclusions are given in Section 5.

2. High order fast algorithm with almost optimum memory of the Caputo fractional derivative. In this section, we consider the high order fast algorithm with almost optimum memory for the evolution of the Caputo fractional derivative, which is defined as in (1.1). Suppose that the time interval $[0, T]$ is covered by a set of grid points $\Omega_t := \{t_n, n = 0, 1, \dots, N_T\}$, with $t_0 = 0, t_{N_T} = T, t_{n+\frac{1}{2}} = \frac{t_n+t_{n+1}}{2}$, and $\Delta t_n = t_n - t_{n-1}$. For simplify, we only consider a uniform distribution of the grid points which means $\Delta t_n = h$ for all n . We will simply denote $u(t_n)$ by u^n . Let us denote the piecewise linear interpolation function of $u(t)$ as $\Pi_{1,h}u(t)$ for any $j \geq 1$, i.e.,

$$\Pi_{1,h}u(t) = u^{j-1} \frac{t_j - t}{h} + u^j \frac{t - t_{j-1}}{h}, \quad \text{for } t \in [t_{j-1}, t_j].$$

Suppose $\Pi_{2,h}u(t)$ be a piecewise quadratic interpolation function of $u(t)$ for $j \geq 2$, which is given as

$$\begin{aligned} \Pi_{2,h}u(t) = & u^{j-2} \frac{(t - t_{j-1})(t - t_j)}{2h^2} + u^{j-1} \frac{(t - t_{j-2})(t_j - t)}{h^2} \\ & + u^j \frac{(t - t_{j-1})(t - t_{j-2})}{2h^2}, \quad \text{for } t \in [t_{j-1}, t_j]. \end{aligned} \quad (2.1)$$

It follows from the interpolation theory that $\Pi_{1,h}u(t)$ and $\Pi_{2,h}u(t)$ have a second-order accuracy and third-order accuracy in time for smooth $u(t)$, respectively. Let us denote $(\Pi_{1,h}u(t))'$ and $(\Pi_{2,h}u(t))'$ as follows

$$(\Pi_{1,h}u(t))' = \delta_t u^{j-\frac{1}{2}}, \quad \text{for } t \in [t_{j-1}, t_j],$$

and

$$(\Pi_{2,h}u(t))' = \delta_t u^{j-\frac{1}{2}} + \delta_t^2 u^{j-1} (t - t_{j-\frac{1}{2}}), \quad \text{for } t \in [t_{j-1}, t_j],$$

respectively. Here $\delta_t u^{j-\frac{1}{2}} = \frac{u^j - u^{j-1}}{h}$ and $\delta_t^2 u^j = \frac{\delta_t u^{j+\frac{1}{2}} - \delta_t u^{j-\frac{1}{2}}}{h}$.

For simplicity, we denote $\Pi_{2,h}u(t) = \Pi_{1,h}u(t)$ for $t \in [t_0, t_1]$. For $0 < \alpha < 1$, the most popular scheme for calculating of the Caputo fractional derivative is called the $L1$ formula [9, 19, 32], whose accuracy is $2 - \alpha$ order in time. In the $L1$ formula, $u(t)$ is replaced by the piecewise linear function $\Pi_{1,h}u(t)$ (as shown in Fig. 2.1-(a)). Another popular high order scheme ($L1 - 2$ formula) achieves $3 - \alpha$ order accuracy [8], in which $u(t)$ is approximated by the linear interpolation function $\Pi_{1,h}u(t)$ at interval $[t_0, t_1]$ and the quadratic interpolation function $\Pi_{2,h}u(t)$ at interval $[t_j, t_{j+1}]$ for $j \geq 1$. It is well known that the $L1$ formula and $L1 - 2$ formula require the storage of all previous function values of u^0, u^1, \dots, u^n and $O(n)$ flops computational cost at the $(n + 1)$ -th time step. For a long time simulation, the direct schemes require very large storage of memory and high computational cost.

Now let us take the Caputo fractional derivative (1.1) as a convolution integral, in which $\frac{1}{(t-\tau)^\alpha}$ can be viewed as a kernel function (weight function). For $0 < \alpha < 1$, the kernel function increases as τ goes from 0 to t . To save memory and computational

cost, a natural idea is to cut the integral by a given integer \bar{S} at the n -th time step, which means

$$\int_0^{t_n} \frac{u'(\tau)}{(t_n - \tau)^\alpha} d\tau \approx \int_{t_{j_0}}^{t_n} \frac{u'(\tau)}{(t_n - \tau)^\alpha} d\tau \approx \sum_{j=j_0+1}^n \delta_t u^{j-\frac{1}{2}} \int_{t_{j-1}}^{t_j} \frac{1}{(t_n - \tau)^\alpha} d\tau, \quad (2.2)$$

where $u(\tau)$ is approximated by $\Pi_{1,h}u(\tau)$ and $j_0 = \max\{0, n - \bar{S}\}$. In the following of the paper, we denote this approximation as the cut off approach (as shown in Fig. 2.1-(b)). It is important to noting that the cut off approach only need limited memory according to the given integer \bar{S} for any large N_T . However, the numerical simulation shows that the accuracy of the cut off approach is unacceptable.

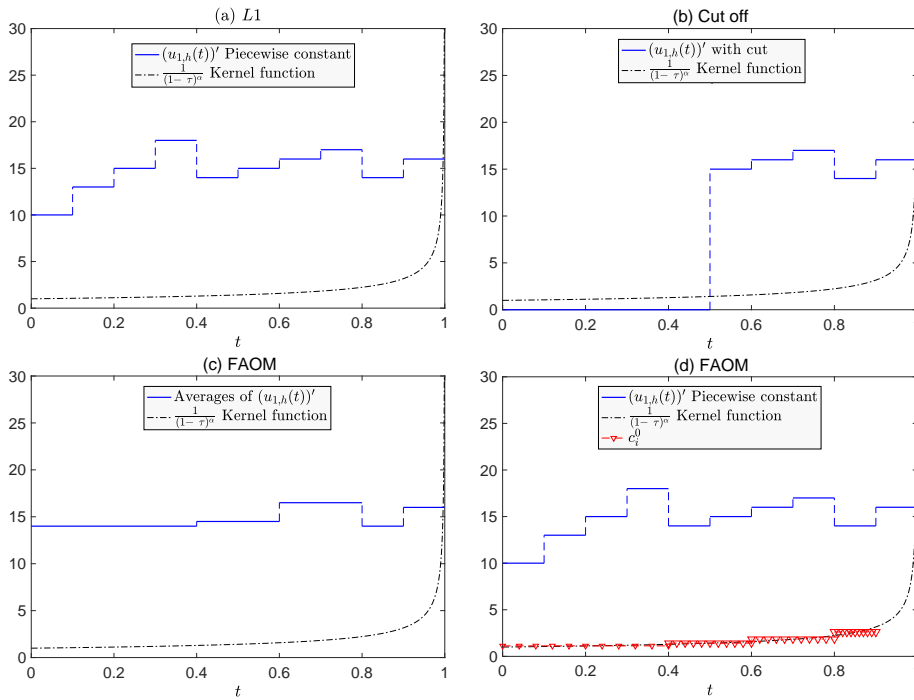


FIG. 2.1. Example for the L1 formula (a), the cut off approximation (b), and the FAOM algorithm (c-d). $T = 1$, $h = 0.1$. In the cut off approximation, $\bar{S} = 5$. $j_1 = 0$, $j_2 = 4$, $j_3 = 6$, $j_4 = 8$, $j_5 = 9$ in the FAOM algorithm.

We next present our fast evaluation method based on the understanding of the L1 formula and the cut off approach. For convenience, we first introduce some useful definitions in here. For any given vector \mathbf{V} , let us define a backward operator \mathcal{B} by $\mathbf{U} = \mathcal{B}(v, \mathbf{V})$ with $U_1 = v$ and $U_i = V_{i-1}$ for $i = 2, 3, \dots, m+1$. Here m is the length of \mathbf{V} . Let \mathcal{F} be a forward operator defined by $\mathbf{U} = \mathcal{F}(M, j, \mathbf{V})$, where $U_i = V_i$ for $i < j$ and $U_i = V_{i+M-1}$ for $i \geq j$ with $M \geq 2$. Let \mathcal{F}_m be a modified forward operator defined by $\mathbf{U} = \mathcal{F}_m(M, j, v, \mathbf{V})$, where $U_i = V_i$ for $i < j$, $U_i = v$ for $i = j$, and $U_i = V_{i+M}$ for $i > j$.

In the cut off approach, the solutions at the previous several time steps are saved since those solutions are important and correspond to large weight functions. However, the numerical simulation suggests that we should take the other solutions into

account, even those solutions correspond to small weight functions. To balance the storage of memory and the accuracy of solution, we save the averages of $(u_{J,h}(\tau))'$ in the nonuniform subintervals $[t_{j_i}, t_{j_{i+1}}]$ in the fast evolution algorithm (as shown in Fig. 2.1-(c)). It is clear that we hope the averages of $(u_{J,h}(\tau))'$ at the previous time steps can be reused in the current time step and the following time steps. Furthermore, the length of the subinterval $[t_{j_i}, t_{j_{i+1}}]$ should decrease as i increases, since the kernel function is an increasing function. By using an interpolation $\Pi_{J,h}u(\tau)$ for $u(t)$, the integral in equation (1.1) at time $t = t_n$ can be approximated as follows

$$\begin{aligned}
\int_0^{t_n} \frac{u'(\tau)}{(t_n - \tau)^\alpha} d\tau &= \int_{t_{n-1}}^{t_n} \frac{u'(\tau)}{(t_n - \tau)^\alpha} d\tau + \int_0^{t_{n-1}} \frac{u'(\tau)}{(t_n - \tau)^\alpha} d\tau := \mathcal{I}_l(t_n) + \mathcal{I}_h(t_n) \\
&\approx \int_{t_{n-1}}^{t_n} \frac{(\Pi_{J,h}u(\tau))'}{(t_n - \tau)^\alpha} d\tau + \int_0^{t_{n-1}} \frac{(\Pi_{J,h}u(\tau))'}{(t_n - \tau)^\alpha} d\tau \\
&\approx \int_{t_{n-1}}^{t_n} \frac{(\Pi_{J,h}u(\tau))'}{(t_n - \tau)^\alpha} d\tau + \sum_i \int_{t_{j_i}}^{t_{j_{i+1}}} \frac{(\Pi_{J,h}u(\tau))'}{t_{j_{i+1}} - t_{j_i}} d\tau \int_{t_{j_i}}^{t_{j_{i+1}}} \frac{1}{(t_n - \tau)^\alpha} d\tau.
\end{aligned} \tag{2.3}$$

Here the integral is decomposed to the local part $\mathcal{I}_l(t_n)$ and the history part $\mathcal{I}_h(t_n)$. The balance between the storage of memory and the accuracy of solution can be done by choosing suitable subintervals $[t_{j_i}, t_{j_{i+1}}]$. It is worth to pointing out that this approximation is the same with the $L1$ formula by setting $t_{j_{i+1}} - t_{j_i} = h$ and $J = 1$. We now propose a fast evolution approach (Algorithm 1) to reach an almost optimum memory by constructing a special sequence of subintervals. The approach is named as the fast algorithm with almost optimum memory (FAOM) of the Caputo fractional derivative.

Algorithm 1: FAOM of the Caputo fractional derivative.

Initialization: Let $\mathbf{U}^n = [U_1^n, U_2^n, \dots, U_{\mathcal{M}_n}^n]$ be a vector, whose elements are the averages of $(u_{J,h}(\tau))'$ on given subintervals, and $\mathbf{I}^n = [I_1^n, I_2^n, \dots, I_{\mathcal{M}_n}^n]$ be a vector, whose elements are the starts of subintervals. Set $\mathbf{U}^0 = 0$ and $\mathbf{I}^0 = 0$. Pre-chosen an integer $\mathcal{N}_\tau \geq 2$ to control the storage of memory.

Start time loop: $t_n = nh$ with $n = 2, 3, \dots, N_T$.

Step 1 (Updating the storage): Update the temporary storage vector by $\tilde{\mathbf{U}}^n =$

$$\mathcal{B}(\tilde{u}_a, \mathbf{U}^{n-1}) \text{ and vector } \tilde{\mathbf{I}}^n = \mathcal{B}(t_{n-2}, \mathbf{I}^{n-1}), \text{ where } \tilde{u}_a = \frac{1}{h} \int_{t_{n-2}}^{t_{n-1}} (\Pi_{J,h}u(\tau))' d\tau.$$

Step 2 (Optimizing of the storage): Obtain the storage vector \mathbf{U}^n and vector \mathbf{I}^n as follows.

- If there exists i_0 such that $\tilde{I}_{i_0}^n - \tilde{I}_{i_0+1}^n = \dots = \tilde{I}_{i_0+2\mathcal{N}_\tau-2}^n - \tilde{I}_{i_0+2\mathcal{N}_\tau-1}^n$, let $\mathbf{I}^n = \mathcal{F}(\mathcal{N}_\tau, i_0 + \mathcal{N}_\tau, \tilde{\mathbf{I}}^n)$ and $\mathbf{U}^n = \mathcal{F}_m(\mathcal{N}_\tau, i_0 + \mathcal{N}_\tau, v, \tilde{\mathbf{U}}^n)$, where $\tilde{I}_0^n = I_0^n = t_{n-1}$ and $v = \frac{1}{\mathcal{N}_\tau} \sum_{i=i_0+\mathcal{N}_\tau}^{i_0+2\mathcal{N}_\tau-1} \tilde{U}_i^n$. Set $\tilde{\mathbf{I}}^n = \mathbf{I}^n$, $\tilde{\mathbf{U}}^n = \mathbf{U}^n$ and redo optimization until there does not exist i_0 satisfying $I_{i_0}^n - I_{i_0+1}^n = \dots = I_{i_0+2\mathcal{N}_\tau-2}^n - I_{i_0+2\mathcal{N}_\tau-1}^n$.

Step 3 (Calculating the Caputo fractional derivative): Approximate the history

part $\mathcal{I}_h(t_n)$ as follows

$$\mathcal{I}_h(t_n) = \int_0^{t_{n-1}} \frac{u'(\tau)}{(t_n - \tau)^\alpha} d\tau \approx \sum_{i=0}^{\mathcal{M}_n-1} U_{i+1}^n \int_{I_{i+1}^n}^{I_i^n} \frac{1}{(t_n - \tau)^\alpha} d\tau, \quad (2.4)$$

where \mathcal{M}_n is the length of the vector \mathbf{U}^n . The numerical Caputo fractional derivative is finally calculated according to (2.3).

End of time loop.

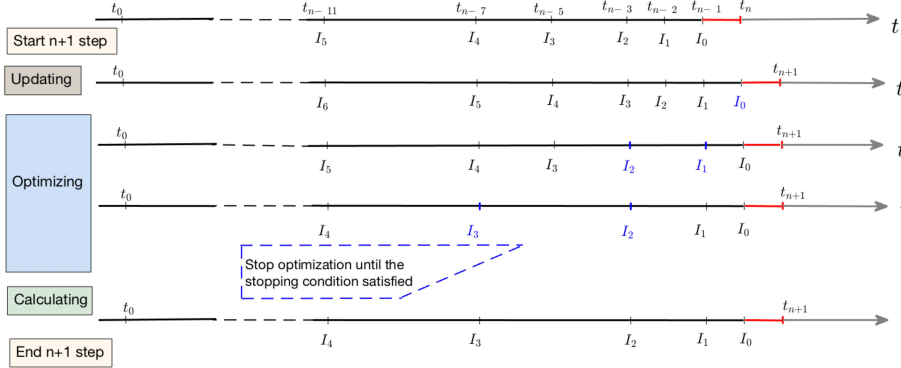


FIG. 2.2. A simple example to explain how we update the vector \mathbf{I}^{n+1} at the $(n+1)$ -th time step. The optimization of the storage vector \mathbf{U}^{n+1} is similar. In this example, we set $\mathcal{N}_\tau = 2$. The part with red color in the time axle is denoted as the local part $\mathcal{I}_l(t_n)$ and the part with black color is denoted as the history part $\mathcal{I}_h(t_n)$.

In the following of the paper, we simplify I_i^n as I_i in the absence of ambiguity. In the FAOM method, the storage requirement and the overall computational cost both are dependent on the number of the nonuniform subintervals, which is equal to the length of the vector \mathbf{U}^n . At the n -th time step, the nonuniform subintervals obtained by the FAOM method satisfy the following properties.

1. The union of all subintervals $(\cup_{i=1}^{\mathcal{M}_n} [I_i, I_{i-1}])$ equals $[0, t_{n-1}]$.
2. The length of the subinterval $[I_i, I_{i-1}]$ is equal to that of the subinterval $[I_{i-1}, I_{i-2}]$ or \mathcal{N}_τ times of it.
3. The length of the subinterval $[I_i, I_{i-1}]$ is $h(\mathcal{N}_\tau)^{K_i}$ with $K_i \in \mathbb{Z}^+$. Here $\{K_i\}_{i=1}^{\mathcal{M}_n}$ is a descending sequence.
4. For any $K_i < K_{\mathcal{M}_n}$, there are at least $\mathcal{N}_\tau - 1$ and at most $2\mathcal{N}_\tau - 2$ subintervals, whose length are $h(\mathcal{N}_\tau)^{K_i}$.
5. Most of the subintervals at the previous time step are unchanged in the current time step.

To further describe the approach clearly, we take a special case as an example and show how the subintervals change from the n -th time step to the $(n+1)$ -th time step in Fig. 2.2. While there are $2\mathcal{N}_\tau - 1$ subintervals with the same length, the FAOM algorithm combines \mathcal{N}_τ of them to a large subinterval during the optimizing step. The following lemmas show the relationship between the length of the vector \mathbf{U}^n and n .

LEMMA 2.1. Let $I_{i-1} - I_i = h(\mathcal{N}_\tau)^{K_i}$ for $i = 1, 2 \dots, \mathcal{M}_n$. The following

inequalities hold

$$\begin{aligned} \frac{i}{2\mathcal{N}_\tau - 2} - 1 &\leq K_i \leq \frac{i-1}{\mathcal{N}_\tau - 1}, \\ \frac{\tau - I_i}{t_n - I_i} &\leq \frac{1}{2}, \quad \forall \tau \in [I_i, I_{i-1}]. \end{aligned} \quad (2.5)$$

Proof. From the second and fourth properties listed above, we obtain that $(\mathcal{N}_\tau)^{i/(2\mathcal{N}_\tau - 2) - 1} \leq \frac{I_{i-1} - I_i}{h} = (\mathcal{N}_\tau)^{K_i} \leq (\mathcal{N}_\tau)^{(i-1)/(\mathcal{N}_\tau - 1)}$ holds for $i \geq 1$, which shows the first inequality in (2.5) holds. From the properties 1, 2, and 4, we get

$$\frac{t_n - I_i}{h} = 1 + \sum_{k=1}^i (\mathcal{N}_\tau)^{K_k} \geq 1 + (\mathcal{N}_\tau)^{K_i} + (\mathcal{N}_\tau - 1) \sum_{k=0}^{K_i-1} (\mathcal{N}_\tau)^k = 2(\mathcal{N}_\tau)^{K_i}, \quad (2.6)$$

which implies $\frac{\tau - I_i}{t_n - I_i} \leq \frac{1}{2}$ holds for any $\tau \in [I_i, I_{i-1}]$. \square

LEMMA 2.2. *At the n -th time step, the length of the vector \mathbf{U}^n satisfies*

$$(\mathcal{N}_\tau - 1)(\log_{\mathcal{N}_\tau} n - 1) \leq \mathcal{M}_n \leq 2(\mathcal{N}_\tau - 1) \log_{\mathcal{N}_\tau} \left(\frac{n+1}{2} \right). \quad (2.7)$$

Proof. At the n -th time step, it is clear $I_1 = t_{n-2}$ and $I_{\mathcal{M}_n} = 0$. Let $[a_{i+1}, a_i]$ be a sequence of intervals with $a_i = I_i/h$ for $i = 0, 1, \dots, \mathcal{M}_n$. According to the properties listed above, we have

$$n - 1 = a_0 - a_{\mathcal{M}_n} = \sum_{i=0}^{\mathcal{M}_n-1} (a_i - a_{i+1}) \leq \sum_{i=0}^{\mathcal{K}} (\mathcal{N}_\tau - 1)(\mathcal{N}_\tau)^i = (\mathcal{N}_\tau)^{\mathcal{K}+1} - 1, \quad (2.8)$$

and the lower bound of \mathcal{M}_n is given by $\mathcal{M}_n \geq (\mathcal{N}_\tau - 1)(\log_{\mathcal{N}_\tau} n - 1)$. Here \mathcal{K} is an integer such that $\frac{\mathcal{M}_n}{\mathcal{N}_\tau - 1} \in (\mathcal{K}, \mathcal{K} + 1]$. On the other hand, we get

$$n - 1 = a_0 - a_{\mathcal{M}_n} = \sum_{i=0}^{\mathcal{M}_n-1} (a_i - a_{i+1}) \geq (2\mathcal{N}_\tau - 2) \sum_{i=0}^{\mathcal{Y}} (\mathcal{N}_\tau)^i = 2[(\mathcal{N}_\tau)^{\mathcal{Y}+1} - 1], \quad (2.9)$$

where \mathcal{Y} is an integer such that $\frac{\mathcal{M}_n}{2\mathcal{N}_\tau - 2} \in (\mathcal{Y}, \mathcal{Y} + 1]$. Then the upper bound of \mathcal{M}_n is given by

$$\mathcal{M}_n \leq 2(\mathcal{N}_\tau - 1) \log_{\mathcal{N}_\tau} \left(\frac{n+1}{2} \right), \quad (2.10)$$

which completes our proof. \square

In the FAOM method, we can choose a small integer number \mathcal{N}_τ to control the storage of memory. Usually, \mathcal{N}_τ is set to be 2 or 3. As compared with the $L1$ approximation, the FAOM method reduces the storage requirement from $O(N_T)$ to $O(\mathcal{N}_\tau \log_{\mathcal{N}_\tau} N_T)$ and the total computational cost from $O(N_T^2)$ to $O(N_T \mathcal{N}_\tau \log_{\mathcal{N}_\tau} N_T)$. Furthermore, the FAOM method will reduce to the $L1$ approximation while $\mathcal{N}_\tau > N_T$. However, the numerical results in the next section show that the convergence order of the FAOM goes to zero while $h \rightarrow 0$. To improve the FAOM method, let us go back to equation (2.3), in which the history part is approximated as

$$\mathcal{I}_h(t_n) \approx \sum_{i=1}^{\mathcal{M}_n} \frac{1}{I_{i-1} - I_i} \int_{I_i}^{I_{i-1}} (\Pi_{J,h} u(\tau))' d\tau \int_{I_i}^{I_{i-1}} \frac{1}{(t_n - \tau)^\alpha} d\tau. \quad (2.11)$$

In the above formula, $u'(\tau)$ is approximated by a constant function on the subinterval $[I_i, I_{i-1}]$. The error of this approximation is dependent on the length of the subinterval $[I_i, I_{i-1}]$. Since the length of subinterval $[I_{\mathcal{M}_n}, I_{\mathcal{M}_{n-1}}]$ does not go to zero as $h \rightarrow 0$, the error of the FAOM method with small \mathcal{N}_τ may not converge to zero as $h \rightarrow 0$. Actually, we can rewrite equation (2.3) as follows

$$\int_0^{t_n} \frac{u'(\tau)}{(t_n - \tau)^\alpha} d\tau \approx \int_{t_{n-1}}^{t_n} \frac{(\Pi_{J,h}u(\tau))'}{(t_n - \tau)^\alpha} d\tau + \sum_{i=1}^{\mathcal{M}_n} c_i^0 \int_{I_i}^{I_{i-1}} (\Pi_{J,h}u(\tau))' d\tau, \quad (2.12)$$

where $c_i^0 = \frac{1}{I_{i-1} - I_i} \int_{I_i}^{I_{i-1}} \frac{1}{(t_n - \tau)^\alpha} d\tau$. In equation (2.12), $u(\tau)$ is approximated by $\Pi_{J,h}u(\tau)$, and the kernel function is replaced by a constant c_i^0 on the subinterval $[I_i, I_{i-1}]$. The difference between the two understandings of the FAOM is shown in Fig. 2.1 (c-d) by a simple example. As shown in Fig. 2.1-(d), the error between the piecewise constant function and the kernel function does not go to zero as $h \rightarrow 0$.

To improve the FAOM method, we introduce a more accurate approximation for the kernel function, which is based on a polynomial approximation of the special function $\frac{1}{(1-\tau)^\alpha}$ on the interval $[-\frac{1}{3}, \frac{1}{3}]$. We denote the new method as the high order fast algorithm with optimum memory based on a K -th degree polynomial approximation (FAOM-PK). Suppose the function $\frac{1}{(1-\tau)^\alpha}$ is approximated by a polynomial function $\sum_{i=0}^K w_i \tau^i$. Let ϵ_K be the absolute error of the approximation, which is defined as follows

$$\left| \frac{1}{(1-\tau)^\alpha} - \sum_{i=0}^K w_i \tau^i \right| \leq \epsilon_K, \quad \tau \in [-\frac{1}{3}, \frac{1}{3}]. \quad (2.13)$$

Next, we propose the FAOM-PK method based on the polynomial approximation. After replacing $u'(\tau)$ by $(\Pi_{J,h}u(\tau))'$, the Caputo fractional derivative is approximated as

$${}_0^C \mathcal{D}_t^\alpha u(t) = \frac{1}{\Gamma(1-\alpha)} \int_{t_{n-1}}^{t_n} \frac{(\Pi_{J,h}u(\tau))'}{(t_n - \tau)^\alpha} d\tau + \frac{1}{\Gamma(1-\alpha)} \int_0^{t_{n-1}} \frac{(\Pi_{J,h}u(\tau))'}{(t_n - \tau)^\alpha} d\tau + \mathcal{R}_{J,h}, \quad (2.14)$$

where $\mathcal{R}_{J,h}$ is the truncation error according to the polynomial approximation of $u(\tau)$. Similar to the FAOM method, we decompose the second integral in the right hand of the above equation into several parts as follows

$$\frac{1}{\Gamma(1-\alpha)} \int_0^{t_{n-1}} \frac{(\Pi_{J,h}u(\tau))'}{(t_n - \tau)^\alpha} d\tau = \frac{1}{\Gamma(1-\alpha)} \sum_{i=0}^{\mathcal{M}_{n-1}} \int_{I_{i+1}}^{I_i} \frac{(\Pi_{J,h}u(\tau))'}{(t_n - \tau)^\alpha} d\tau. \quad (2.15)$$

By setting $I_{i+\frac{1}{2}} = (I_i + I_{i+1})/2$ and $\bar{\tau} = \tau - I_{i+\frac{1}{2}}$, the $(i+1)$ -th term in the right hand of (2.15) can be rewritten as

$$\frac{1}{\Gamma(1-\alpha)} \int_{I_{i+1}}^{I_i} \frac{(\Pi_{J,h}u(\tau))'}{(t_n - \tau)^\alpha} d\tau = \frac{1}{\Gamma(1-\alpha)} \int_{I_{i+1} - I_{i+\frac{1}{2}}}^{I_i - I_{i+\frac{1}{2}}} \frac{(\Pi_{J,h}u(I_{i+\frac{1}{2}} + \bar{\tau}))'}{(t_n - I_{i+\frac{1}{2}} - \bar{\tau})^\alpha} d\bar{\tau}. \quad (2.16)$$

After denoting $\tilde{\tau} = \frac{\bar{\tau}}{t_n - I_{i+\frac{1}{2}}}$, the kernel function $(t_n - I_{i+\frac{1}{2}} - \bar{\tau})^{-\alpha}$ in (2.16) is equal to $(t_n - I_{i+\frac{1}{2}})^{-\alpha} \frac{1}{(1-\tilde{\tau})^\alpha}$. Thanks to Lemma 2.1, we have $-\frac{1}{3} \leq \tilde{\tau} \leq \frac{1}{3}$ holds for all $\tau \in [I_{i+1}, I_i]$. Using the polynomial approximation of the function $\frac{1}{(1-\tilde{\tau})^\alpha}$, the $(i+1)$ -th term in the right hand of (2.15) can be approximated as

$$\frac{1}{\Gamma(1-\alpha)} \int_{I_{i+1}}^{I_i} \frac{(\Pi_{J,h}u(\tau))'}{(t_n - \tau)^\alpha} d\tau = \sum_{k=0}^K \frac{\bar{w}_k^i}{\Gamma(1-\alpha)} \int_{I_{i+1}}^{I_i} (\Pi_{J,h}u(\tau))' \left(\frac{\tau - I_{i+\frac{1}{2}}}{I_i - I_{i+\frac{1}{2}}} \right)^k d\tau + \mathcal{R}_K^i, \quad (2.17)$$

where $\bar{w}_k^i = w_k \frac{(I_i - I_{i+\frac{1}{2}})^k}{(t_n - I_{i+\frac{1}{2}})^{k+\alpha}}$ and \mathcal{R}_K^i denotes the cut off error according to the polynomial approximation of $\frac{1}{(1-\tilde{\tau})^\alpha}$. By combining (2.14), (2.15), and (2.17), the numerical scheme of the Caputo fractional derivative is finally given as follows

$$\begin{aligned} {}_0^C \mathcal{D}_t^\alpha u(t) &= \int_0^{t_n} \frac{u'(\tau)}{(t_n - \tau)^\alpha} d\tau = \frac{1}{\Gamma(1-\alpha)} \int_{t_{n-1}}^{t_n} \frac{(\Pi_{J,h}u(\tau))'}{(t_n - \tau)^\alpha} d\tau \\ &+ \sum_{i=0}^{\mathcal{M}_n-1} \sum_{k=0}^K \frac{\bar{w}_k^i}{\Gamma(1-\alpha)} \int_{I_{i+1}}^{I_i} (\Pi_{J,h}u(\tau))' \left(\frac{\tau - I_{i+\frac{1}{2}}}{I_i - I_{i+\frac{1}{2}}} \right)^k d\tau + \mathcal{R}_K + \mathcal{R}_{J,h} \\ &:= {}_0^C \mathcal{D}_t^{F,\alpha} u(t) + \mathcal{R}_K + \mathcal{R}_{J,h}, \end{aligned} \quad (2.18)$$

where ${}_0^C \mathcal{D}_t^{F,\alpha} u(t)$ presents the numerical Caputo fractional derivative calculated by the FAOM-PK method. Here $\mathcal{R}_K = \sum_{i=0}^{\mathcal{M}_n-1} \mathcal{R}_K^i$ denotes the total truncation error according to the polynomial approximation of $\frac{1}{(1-\tilde{\tau})^\alpha}$.

In the FAOM-PK method, we save $\int_{I_{i+1}}^{I_i} (\Pi_{J,h}u(\tau))' \left(\frac{\tau - I_{i+1/2}}{I_i - I_{i+1/2}} \right)^k d\tau$, $k = 0, 1, \dots, K$ at each time step. The total memory requirement in the FEOM-PK method is $O((K+1)\mathcal{N}_\tau \log_{\mathcal{N}_\tau} n)$ at the n -th time step. During the optimizing step, the \mathcal{N}_τ subintervals with the same length is combined to a large one. At the same time, the corresponding integrals we saved also need to be combined. In the case of $I_i - I_{i+1} = I_{i+1} - I_{i+2} = \dots = I_{i+\mathcal{N}_\tau-1} - I_{i+\mathcal{N}_\tau}$, the integrals on the subinterval $[I_{i+\mathcal{N}_\tau}, I_i]$ can be decomposed as follows

$$\begin{aligned} \int_{I_{i+\mathcal{N}_\tau}}^{I_i} (\Pi_{J,h}u(\tau))' \left(\frac{\tau - I_{i+\mathcal{N}_\tau/2}}{I_i - I_{i+\mathcal{N}_\tau/2}} \right)^k d\tau &= \sum_{j=0}^{\mathcal{N}_\tau-1} \int_{I_{i+j+1}}^{I_{i+j}} (\Pi_{J,h}u(\tau))' \left(\frac{\tau - I_{i+\mathcal{N}_\tau/2}}{I_i - I_{i+\mathcal{N}_\tau/2}} \right)^k d\tau \\ &= \sum_{j=0}^{\mathcal{N}_\tau-1} \int_{I_{i+j+1}}^{I_{i+j}} (\Pi_{J,h}u(\tau))' \left(\frac{\tau - I_{i+j+\frac{1}{2}}}{\mathcal{N}_\tau(I_{i+j} - I_{i+j+\frac{1}{2}})} - \frac{2j+1-\mathcal{N}_\tau}{\mathcal{N}_\tau} \right)^k d\tau \\ &= \sum_{j=0}^{\mathcal{N}_\tau-1} \sum_{l=0}^k \frac{C_k^l}{\mathcal{N}_\tau^k} (\mathcal{N}_\tau - 2j - 1)^{k-l} \int_{I_{i+j+1}}^{I_{i+j}} (\Pi_{J,h}u(\tau))' \left(\frac{\tau - I_{i+j+\frac{1}{2}}}{I_{i+j} - I_{i+j+\frac{1}{2}}} \right)^l d\tau, \end{aligned} \quad (2.19)$$

which gives a rule for optimizing the storage. The FAOM-PK algorithm is finally given in Algorithm 2.

Algorithm 2: FAOM-PK of the Caputo fractional derivative.

Initialization: Let $\mathbf{I}^n = [I_1^n, I_2^n, \dots, I_{\mathcal{M}_n}^n]$ be a vector, whose elements are the starts of subintervals, and $\mathbf{U}^{n,k} = [U_1^{n,k}, U_2^{n,k}, \dots, U_{\mathcal{M}_n}^{n,k}]$ with $k = 0, 1, \dots, K$, be vectors, whose elements are $\int_{I_i}^{I_{i-1}} (\Pi_{J,h} u(\tau))' \left(\frac{\tau - I_{i-1/2}}{I_{i-1} - I_{i-1/2}} \right)^k d\tau$, respectively. Set $\mathbf{U}^{0,k} = 0$ and $\mathbf{I}^0 = 0$. Pre-chosen an integer number $\mathcal{N}_\tau \geq 2$ to control the storage of memory.

Start time loop: $t_n = nh$ with $n = 2, 3, \dots, N_T$.

Step 1 (Updating the storage): Update the temporary vector $\tilde{\mathbf{I}}^n = \mathcal{B}(t_{n-2}, \mathbf{I}^{n-1})$ and the temporary storage vectors by $\tilde{\mathbf{U}}^{n,k} = \mathcal{B} \left(\int_{t_{n-2}}^{t_{n-1}} (\Pi_{J,h} u(\tau))' \left(\frac{\tau - t_{n-3/2}}{h/2} \right)^k d\tau, \mathbf{U}^{n-1,k} \right)$.

Step 2 (Optimizing of the storage): Obtain the storage vectors $\mathbf{U}^{n,k}$ and vector \mathbf{I}^n as follows.

- If there exists i_0 such that $\tilde{I}_{i_0}^n - \tilde{I}_{i_0+1}^n = \dots = \tilde{I}_{i_0+2\mathcal{N}_\tau-2}^n - \tilde{I}_{i_0+2\mathcal{N}_\tau-1}^n$, let $\mathbf{U}^n = \mathcal{F}(\mathcal{N}_\tau, i_0 + \mathcal{N}_\tau, v, \tilde{\mathbf{U}}^n)$ and $\mathbf{I}^n = \mathcal{F}(\mathcal{N}_\tau, i_0 + \mathcal{N}_\tau, \tilde{\mathbf{I}}^n)$. Here $I_0^n = \tilde{I}_0^n = t_{n-1}$ and $v = \int_{\tilde{I}_{i_0+2\mathcal{N}_\tau-1}}^{\tilde{I}_{i_0+\mathcal{N}_\tau-1}} (\Pi_{J,h} u(\tau))' \left(\frac{\tau - I_{i-1/2}}{I_{i-1} - I_{i-1/2}} \right)^k d\tau$ is calculated according to (2.19). Set $\tilde{\mathbf{I}}^n = \mathbf{I}^n$, $\tilde{\mathbf{U}}^{n,k} = \mathbf{U}^{n,k}$ and redo optimization until there does not exist i_0 such that $I_{i_0}^n - I_{i_0+1}^n = \dots = I_{i_0+2\mathcal{N}_\tau-2}^n - I_{i_0+2\mathcal{N}_\tau-1}^n$ are satisfied.

Step 3 (Calculating the Caputo fractional derivative): Obtain the numerical Caputo fractional derivative according to (2.18).

End of time loop.

The truncation error of the FAOM-PK algorithm can be decomposed into two parts, which are \mathcal{R}_K and $\mathcal{R}_{J,h}$. Here \mathcal{R}_K is the total truncation error according to the polynomial approximation of the kernel function and $\mathcal{R}_{J,h}$ is the truncation error according to the polynomial interpolation of $u(t)$. It is worth to pointing out that the two parts are independent. The estimate of the truncation error $\mathcal{R}_{J,h}$, according to the $L1$ or $L1 - 2$ polynomial interpolation of $u(t)$, can be founded in [8, 32]. The following Lemma, which can be found in [32], establishes an error bound for the $L1$ formula.

LEMMA 2.3. *Suppose $u(t) \in C^2[0, t_n]$. For any α ($0 < \alpha < 1$), then*

$$|\mathcal{R}_{1,h}| \leq \frac{1}{1-\alpha} \left[\frac{1-\alpha}{12} + \frac{2^{2-\alpha}}{2-\alpha} - (1+2^{-\alpha}) \right] \max_{0 \leq t \leq t_n} |u''(t)| h^{2-\alpha}. \quad (2.20)$$

The truncation error of $L1 - 2$ formula is illustrated in the following Lemma, which can be found in [8].

LEMMA 2.4. Suppose $u(t) \in C^3[0, t_n]$. For any α ($0 < \alpha < 1$), then

$$|\mathcal{R}_{2,h}| \leq \begin{cases} \frac{\alpha}{2\Gamma(3-\alpha)} \max_{0 \leq t \leq t_1} |u''(t)| h^{2-\alpha}, & n = 1, \\ \frac{1}{\Gamma(1-\alpha)} \left\{ \frac{\alpha}{12} \max_{0 \leq t \leq t_1} |u''(t)| (t_n - t_1)^{-\alpha-1} h^3 + \left[\frac{1}{12} \right. \right. \\ \left. \left. + \frac{\alpha}{3(1-\alpha)(2-\alpha)} \left(\frac{1}{2} + \frac{1}{3-\alpha} \right) \right] \max_{0 \leq t \leq t_n} |u'''(t)| h^{3-\alpha} \right\}, & n \geq 2. \end{cases} \quad (2.21)$$

The following two Lemmas establish an error bound for \mathcal{R}_K .

LEMMA 2.5. At the n -th time step, the following inequality is satisfied

$$\left| \left(\frac{t_n - I_{i+\frac{1}{2}}}{t_n - \tau} \right)^\alpha - \sum_{k=0}^K w_k \left(\frac{\tau - I_{i+\frac{1}{2}}}{t_n - I_{i+\frac{1}{2}}} \right)^k \right| \leq \epsilon_K, \quad \forall \tau \in [I_{i+1}, I_i]. \quad (2.22)$$

Proof. From Lemma 2.1, we have $\frac{\tau - I_{i+1}}{t_n - I_{i+1}} \leq \frac{1}{2}$ holds for all $\tau \in [I_{i+1}, I_i]$, which implies $t_n - I_{i+\frac{1}{2}} \geq 3(I_i - I_{i+\frac{1}{2}})$. Then we obtain $\left| \frac{\tau - I_{i+\frac{1}{2}}}{t_n - I_{i+\frac{1}{2}}} \right| \leq \frac{1}{3}$ holds for all $\tau \in [I_{i+1}, I_i]$. Thanks to (2.13), the following inequality holds for all $\tau \in [I_{i+1}, I_i]$

$$\left| \left(\frac{t_n - I_{i+\frac{1}{2}}}{t_n - \tau} \right)^\alpha - \sum_{k=0}^K w_k \bar{\tau}^k \right| = \left| \frac{1}{(1 - \bar{\tau})^\alpha} - \sum_{k=0}^K w_k \bar{\tau}^k \right| \leq \epsilon_K, \quad (2.23)$$

where $\bar{\tau} = \frac{\tau - I_{i+\frac{1}{2}}}{t_n - I_{i+\frac{1}{2}}}$. The proof of the Lemma is completed. \square

LEMMA 2.6. Suppose $u(t) \in C^1[0, t_n]$. At the n -th time step, the total cut off error according to the polynomial approximation \mathcal{R}_K is bounded by

$$|\mathcal{R}_K| \leq C \epsilon_K t_n^{1-\alpha} \max_{0 \leq t \leq t_n} |u'(t)|, \quad (2.24)$$

where C is a constant independent of h and ϵ_K .

Proof. From Lemma 2.5 and (2.17), we have

$$\begin{aligned} |\mathcal{R}_K^i| &= \frac{1}{\Gamma(1-\alpha)} \left| \int_{I_{i+1}}^{I_i} \frac{(\Pi_{J,h} u(\tau))'}{(t_n - I_{i+\frac{1}{2}})^\alpha} \left(\left(\frac{t_n - I_{i+\frac{1}{2}}}{t_n - \tau} \right)^\alpha - \sum_{k=0}^K w_k^i \left(\frac{\tau - I_{i+\frac{1}{2}}}{t_n - I_{i+\frac{1}{2}}} \right)^k \right) d\tau \right| \\ &\leq C \epsilon_K \frac{I_i - I_{i+1}}{(t_n - I_{i+\frac{1}{2}})^\alpha} \max_{I_{i+1} \leq t \leq I_i} |u'(t)| \\ &\leq C \epsilon_K (I_i - I_{i+1})^{1-\alpha} \max_{I_{i+1} \leq t \leq I_i} |u'(t)|, \end{aligned} \quad (2.25)$$

where C is a constant independent of h and ϵ_K . By taking the summation of the above equations from 0 to $\mathcal{M}_n - 1$, it follows that the bound of the total truncation error according to the polynomial approximation \mathcal{R}_K is given by

$$|\mathcal{R}_K| \leq C \epsilon_K t_n^{1-\alpha} \max_{0 \leq t \leq t_n} |u'(t)|. \quad (2.26)$$

Here C is a constant independent of h and ϵ_K . \square

THEOREM 2.1. *Suppose $u(t) \in C^{J+1}[0, t_n]$. For any α ($0 < \alpha < 1$), the gap between the Caputo fractional derivative ${}^C_0\mathcal{D}_t^\alpha u(t)$ and the numerical Caputo fractional derivative ${}^C_0\mathcal{D}_t^{F,\alpha} u(t)$ satisfies*

$$\left| {}^C_0\mathcal{D}_t^\alpha u(t) - {}^C_0\mathcal{D}_t^{F,\alpha} u(t) \right| \leq \mathcal{R}_{J,h} + C\epsilon_K t_n^{1-\alpha} \max_{0 \leq t \leq t_n} |u'(t)|, \quad (2.27)$$

where C is a constant independent of h and ϵ_K .

By combining the above Lemmas, we can prove Theorem 2.1 easily. As shown in Theorem 2.1, the FAOM-PK method should have the same order of convergence rate as the corresponding direct method with small ϵ_K . Numerical results in the next two sections show that $\epsilon_K \approx 1e-3$ with $K = 4$ is good enough corresponding to $L1$ approach and $\epsilon_K \approx 1e-6$ with $K = 9$ is good enough corresponding to $L1 - 2$ formula, respectively. From Theorem 2.1, we conclude that the fast algorithm FAOM-PK can be used together with any direct scheme with polynomial interpolation of $u(t)$.

3. Validity of the proposed methods. In this section, we validate the proposed methods and study the convergence rates. Let us consider the following pure initial value problem of the linear fractional diffusion equation

$$\begin{aligned} {}^C_0\mathcal{D}_t^\alpha u(x, t) &= u_{xx}(x, t) + f(x, t) & x \in \Omega_x, \quad t > 0, \\ u(x, 0) &= u_0(x) & x \in \Omega_x, \\ u(x, t) &= \varphi(x, t) & x \in \partial\Omega_x, \quad t > 0, \end{aligned} \quad (3.1)$$

where the domain $\Omega_x = [a, b]$. Suppose the domain Ω_x is covered by a uniform mesh with $\Delta x = \frac{b-a}{N}$. The set of all mesh points is denoted as $\Omega_x^{\Delta x} = \{x_i, i = 0, 1, \dots, N\}$, with $x_i = a + i\Delta x$. We will simply denote the approximation of $u(x_i, t_j)$ by u_i^j . In this section, we consider a second-order and a fourth-order finite difference scheme to discretize the spatial derivative u_{xx} , respectively. In the second-order finite difference scheme, u_{xx} is discretized by the central scheme as follows

$$u_{xx}(x_i, t_j) \approx \frac{u_{i+1}^j + u_{i-1}^j - 2u_i^j}{\Delta x^2}. \quad (3.2)$$

The fourth-order finite difference scheme we used is proposed in [10], which is a compact difference scheme and achieves fourth-order accuracy in space. In this section, a test case is studied to validate the proposed methods.

Example 3.1. In (3.1), we set the computational domain $\Omega_x = [0, \pi]$. The source term $f(x, t)$, the initial data $u_0(x)$, and the boundary value $\varphi(x, t)$ are given by

$$\begin{aligned} f(x, t) &= \Gamma(4 + \alpha)x^4(\pi - x)^4 \exp(-x)t^3/6 - x^2(\pi - x)^2 \{t^{3+\alpha} \exp(-x) \\ &\quad [x^2(56 - 16x + x^2) - 2\pi x(28 - 12x + x^2) + \pi^2(12 - 8x + x^2)] \\ &\quad + 4(3\pi^2 - 14\pi x + 14x^2)\} & x \in \Omega_x, \quad t \in (0, T], \\ u_0(x) &= x^4(\pi - x)^4 & x \in \Omega_x, \\ \varphi(x, t) &= x^4(\pi - x)^4 [\exp(-x)t^{3+\alpha} + 1] & x \in \partial\Omega_x, \quad t \in (0, T]. \end{aligned} \quad (3.3)$$

It is clear that the linear problem (3.1) has the following exact solution

$$u(x, t) = x^4(\pi - x)^4 [\exp(-x)t^{3+\alpha} + 1] \quad x \in \Omega_x, \quad t \in [0, T]. \quad (3.4)$$

To test the accuracy of our schemes, we define the maximum norm of the error and the convergence rates with respect to temporal and spatial mesh sizes, which are given as follows

$$E(\Delta x, h) = \sqrt{h \sum_{j=1}^{N_T} \|e^j\|_\infty^2}, \quad r_s = \log_2 \frac{E(\Delta x, h)}{E(\Delta x/2, h)}, \quad r_t = \log_2 \frac{E(\Delta x, h)}{E(\Delta x, h/2)},$$

where the error $e_i^j = u(x_i, t_j) - u_i^j$.

To understand the accuracy of the FAOM method and the FAOM-PK method in time, we run the code with different time step sizes $h = 1/10, 1/20, 1/40, 1/80, 1/160$, and a fixed spatial mesh size $\Delta x = \pi/20000$. For comparison, we also simulate the example by the cut off approach, $L1$ formula, $L1 - 2$ formula, and a fast method proposed in [11]. The computational errors and numerical convergence rates for different methods with $\alpha = 0.9, 0.5, 0.1$ are given in Tables 3.1 and 3.2. The results reported in Table 3.1 show that the error of cut off approach increases as the time step size decrease. However, the FAOM method achieves bounded errors for all time step sizes we used, even the storages of memory for the two methods are almost the same. As reported in the tables, the $L1$ formula and $L1 - 2$ formula both reach the ideal convergence orders, which are $2 - \alpha$ and $3 - \alpha$, respectively. We also find that the accuracy of the FAOM-PK method is as good as the $L1$ formula and $L1 - 2$ formula, if the same interpolation function $\Pi_{J,h}u(t)$ is used. All results are consistent with our analysis given in the previous section. In the paper, the polynomial approximation of the kernel function $\frac{1}{(1-\tau)^\alpha}$ is given by the Taylor expansion.

To check the convergence rate of our FAOM-PK method in space, we do the simulations with different spatial mesh sizes $\Delta x = \pi/20, \pi/40, \pi/80, \pi/160, \pi/320$ and a fixed time step size $h = 0.001$. Two simulations with $\alpha = 0.5$ are considered. In the first one, $u(t)$ is approximated by $\Pi_{1,h}u(t)$ and u_{xx} is discretized by the second-order finite difference scheme. In the second simulation, $u(t)$ is approximated by $\Pi_{2,h}u(t)$ and u_{xx} is discretized by the fourth-order compact finite difference scheme. As shown in Fig. 3.1, the FAOM-PK can reach the ideal convergence order in space for the two finite difference schemes.

We then investigate the long time performance of FAOM-PK method. We compute the example until $T = 10$ with $h = 0.01$ and $\Delta x = \pi/20000$. Four different methods are considered, which are $L1$ formula, $L1 - 2$ formula, the fast method proposed in [11], and the FAOM-PK method, respectively. We focus on the accuracy and memory usage of those methods. As plotted in Fig. 3.2-(a), the the FAOM-PK method and the fast method proposed in [11] can reach the same accuracy with the $L1$ formula. Furthermore, the high order FAOM-PK algorithm also has similar accuracy as compared with the $L1 - 2$ formula. We plot the length of vector \mathbf{U}^n as a function of n in Fig. 3.2-(b), from which we clearly see that \mathcal{M}_n is between $\log_2 n - 1$ and $2\log_2 \frac{n+1}{2}$. The relationship verifies the Lemma 2.2 and shows that the storage of memory for the FAOM-PK algorithm is $O((K+1)\mathcal{N}_\tau \log_{\mathcal{N}_\tau} n)$ at each time step. As a function of total time steps N_T , the total computational times of the direct methods and the FAOM-PK method are plotted in Fig. 3.2-(c-d). We observe that the total compute time increases almost linearly with the total number of time steps N_T for the FAOM-PK method, but the total compute time for the direct scheme is in the order of $O(N_T^2)$. There is a significant speed-up in the FAOM-PK algorithm as compared with the direct schemes.

TABLE 3.1

The errors and convergence orders in time with fixed spatial mesh size $\Delta x = \pi/20000$ for the proposed methods. In all methods, $u(t)$ is approximated by $\Pi_{1,h}u(t)$, and the second-order finite difference scheme is used. $T = 1$, $\mathcal{N}_\tau = 2$, $\bar{S} = 10$. In the FAOM-PK method, we choose $K = 4$ such that $\epsilon_K \approx 1e-3$. Here “JIANG” denotes the fast algorithm presented in [11].

| h | Cut off | | FAOM | | $L1$ formula | | JIANG | | FAOM-P4 | |
|----------------|-------------------|-------|-------------------|-------|-------------------|-------|-------------------|-------|-------------------|-------|
| | $E(\cdot, \cdot)$ | r_t | $E(\cdot, \cdot)$ | r_t | $E(\cdot, \cdot)$ | r_t | $E(\cdot, \cdot)$ | r_t | $E(\cdot, \cdot)$ | r_t |
| $\alpha = 0.9$ | | | | | | | | | | |
| 1/10 | 3.66e-1 | - | 3.69e-1 | 1.16 | 3.66e-1 | 1.17 | 3.66e-1 | 1.17 | 3.66e-1 | 1.17 |
| 1/20 | 1.66e-1 | - | 1.65e-1 | 1.11 | 1.62e-1 | 1.14 | 1.62e-1 | 1.14 | 1.62e-1 | 1.14 |
| 1/40 | 1.06e-1 | - | 7.66e-2 | 1.05 | 7.39e-2 | 1.12 | 7.39e-2 | 1.12 | 7.39e-2 | 1.12 |
| 1/80 | 1.34e-1 | - | 3.69e-2 | 0.97 | 3.41e-2 | 1.11 | 3.41e-2 | 1.11 | 3.41e-2 | 1.11 |
| 1/160 | 2.16e-1 | - | 1.89e-2 | - | 1.58e-2 | - | 1.58e-2 | - | 1.58e-2 | - |
| $\alpha = 0.5$ | | | | | | | | | | |
| 1/10 | 7.59e-2 | - | 8.22e-2 | 1.28 | 7.59e-2 | 1.48 | 7.60e-2 | 1.48 | 7.60e-2 | 1.48 |
| 1/20 | 6.10e-2 | - | 3.38e-2 | 1.02 | 2.73e-2 | 1.47 | 2.73e-2 | 1.47 | 2.73e-2 | 1.47 |
| 1/40 | 2.45e-1 | - | 1.67e-2 | 0.63 | 9.83e-3 | 1.48 | 9.84e-3 | 1.47 | 9.85e-3 | 1.47 |
| 1/80 | 6.11e-1 | - | 1.08e-2 | 0.27 | 3.54e-3 | 1.48 | 3.54e-3 | 1.48 | 3.56e-3 | 1.47 |
| 1/160 | 1.11 | - | 8.97e-3 | - | 1.27e-3 | - | 1.27e-3 | - | 1.29e-3 | - |
| $\alpha = 0.1$ | | | | | | | | | | |
| 1/10 | 5.35e-3 | - | 7.50e-3 | 1.03 | 5.35e-3 | 1.76 | 5.35e-2 | 1.76 | 5.35e-2 | 1.76 |
| 1/20 | 1.10e-1 | - | 3.68e-3 | 0.46 | 1.58e-3 | 1.77 | 1.58e-3 | 1.77 | 1.58e-3 | 1.76 |
| 1/40 | 4.91e-1 | - | 2.67e-3 | 0.11 | 4.63e-4 | 1.78 | 4.64e-4 | 1.77 | 4.65e-4 | 1.77 |
| 1/80 | 1.05 | - | 2.47e-3 | - | 1.35e-4 | 1.79 | 1.36e-4 | 1.77 | 1.36e-4 | 1.76 |
| 1/160 | 1.61 | - | 2.48e-3 | - | 3.90e-5 | - | 3.99e-5 | - | 4.00e-5 | - |

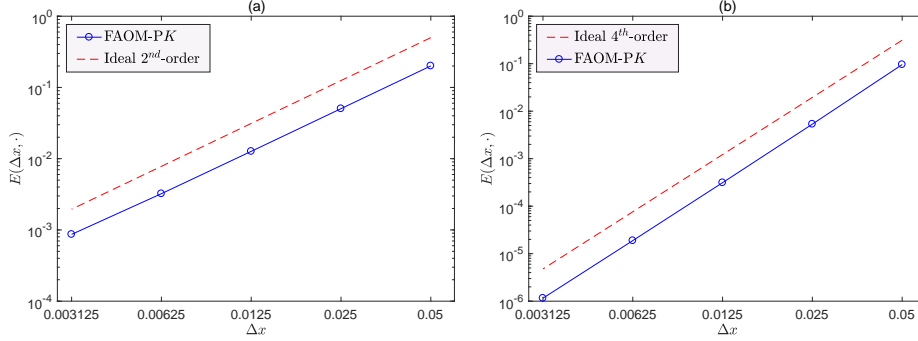


FIG. 3.1. The errors in space with fixed time step size $h = 0.001$ for the proposed methods and $T = 1$. (a) $u(t)$ is approximated by $\Pi_{1,h}u(t)$, the second-order finite difference scheme is used to discretize u_{xx} , and $K = 4$; (b) $u(t)$ is approximated by $\Pi_{2,h}u(t)$, the fourth-order compact finite difference scheme is used to discretize u_{xx} , and $K = 9$.

4. Nonlinear fractional diffusion equation. We now consider the initial value problem of the nonlinear fractional diffusion equation as follows

$$\begin{aligned}
{}^C D_t^\alpha u(x, t) &= u_{xx}(x, t) + f(u) + g(x, t) & x \in \Omega_x, t > 0, \\
u(x, 0) &= u_0(x) & x \in \Omega_x, \\
u(x, t) &= \varphi(x, t) & x \in \partial\Omega_x, t > 0.
\end{aligned} \tag{4.1}$$

TABLE 3.2

The errors and convergence orders in time with fixed spatial mesh size $\Delta x = \pi/20000$ for the proposed methods. In all methods, $u(t)$ is approximated by $\Pi_{2,h}u(t)$, and the fourth-order compact finite difference scheme is used. $T = 1$, $\mathcal{N}_\tau = 2$. In the FAOM-PK method, we choose $K = 9$ such that $\epsilon_K \approx 1e-6$.

| | h | L1 - 2 | | FAOM-P9 | |
|----------------|-------|-------------------|-------|-------------------|-------|
| | | $E(\cdot, \cdot)$ | r_t | $E(\cdot, \cdot)$ | r_t |
| $\alpha = 0.9$ | 1/10 | 6.30e-2 | 2.06 | 6.30e-2 | 2.06 |
| | 1/20 | 1.51e-2 | 2.08 | 1.51e-2 | 2.08 |
| | 1/40 | 3.57e-3 | 2.09 | 3.57e-3 | 2.09 |
| | 1/80 | 8.39e-4 | 2.09 | 8.39e-4 | 2.09 |
| | 1/160 | 1.96e-4 | - | 1.96e-2 | - |
| $\alpha = 0.5$ | 1/10 | 1.03e-2 | 2.44 | 1.02e-2 | 2.44 |
| | 1/20 | 1.89e-3 | 2.46 | 1.89e-3 | 2.46 |
| | 1/40 | 3.44e-4 | 2.47 | 3.44e-4 | 2.47 |
| | 1/80 | 6.21e-5 | 2.48 | 6.21e-5 | 2.48 |
| | 1/160 | 1.11e-5 | - | 1.11e-5 | - |
| $\alpha = 0.1$ | 1/10 | 5.59e-4 | 2.76 | 5.54e-4 | 2.76 |
| | 1/20 | 8.24e-5 | 2.77 | 8.20e-5 | 2.77 |
| | 1/40 | 1.20e-5 | 2.94 | 1.20e-5 | 2.94 |
| | 1/80 | 1.57e-6 | 2.45 | 1.57e-6 | 2.45 |
| | 1/160 | 2.88e-7 | - | 2.88e-7 | - |

In this section, we focus on the discretization of the fractional diffusion derivative and discretize the spatial derivative u_{xx} by the second-order finite difference scheme given in (3.2). To complete the discretization of the nonlinear fractional diffusion equation, it still needs to consider the approximation of $f(u)$. If we treat this term implicitly, a nonlinear algebraic system is constructed and needs to be solved at each time step. This may lead extra computational cost and make the algorithm complicated. In [11, 15], $f(u(x_i, t_{j+1}))$ is explicitly approximated as $f(u_i^j)$ at the $(j+1)$ -th time step. This explicit approximation is high efficient and easily implemented. However, the method only enjoys a first-order accuracy in time even L1 formula is used [11, 15]. This is because the accuracy of the approximation $u^{j+1} \approx u^j$ is only first-order. In this paper, we treat $f(u)$ explicitly with a high order approximation of u^{j+1} by the solution of the previous several time steps. At the $(j+1)$ -th time step, the discrete scheme for nonlinear fractional diffusion equation (4.1) is given as follows

$$\begin{aligned}
C_0 \mathcal{D}_t^{F,\alpha} u_i^{j+1} &= \frac{u_{i+1}^{j+1} + u_{i-1}^{j+1} - 2u_i^{j+1}}{\Delta x^2} + f(\tilde{u}_i^{j+1}) + g(x_i, t_{j+1}) \quad 1 \leq i \leq N-1, \\
u_i^0 &= u_0(x_i) \quad 0 \leq i \leq N, \\
u_i^{j+1} &= \varphi(x_i, t_{j+1}) \quad i = 0 \text{ or } i = N,
\end{aligned} \tag{4.2}$$

where \tilde{u}_i^{j+1} is a high order approximation of u_i^{j+1} . In this paper, \tilde{u}_i^{j+1} equals $2u_i^j - u_i^{j-1}$ with $j > 0$ and $\tilde{u}_i^1 = u_i^0$ for L1 approach. For L1 - 2 approach, \tilde{u}_i^{j+1} equals $3u_i^j - 3u_i^{j-1} + u_i^{j-2}$ for $j > 1$, $\tilde{u}_i^2 = 2u_i^1 - u_i^0$, and $\tilde{u}_i^1 = u_i^0$.

Example 4.1. In (4.1), we assume the computational domain $\Omega_x = [0, \pi]$. The nonlinear term $f(u)$, the source term $g(x, t)$, the initial data $u_0(x)$, and the boundary

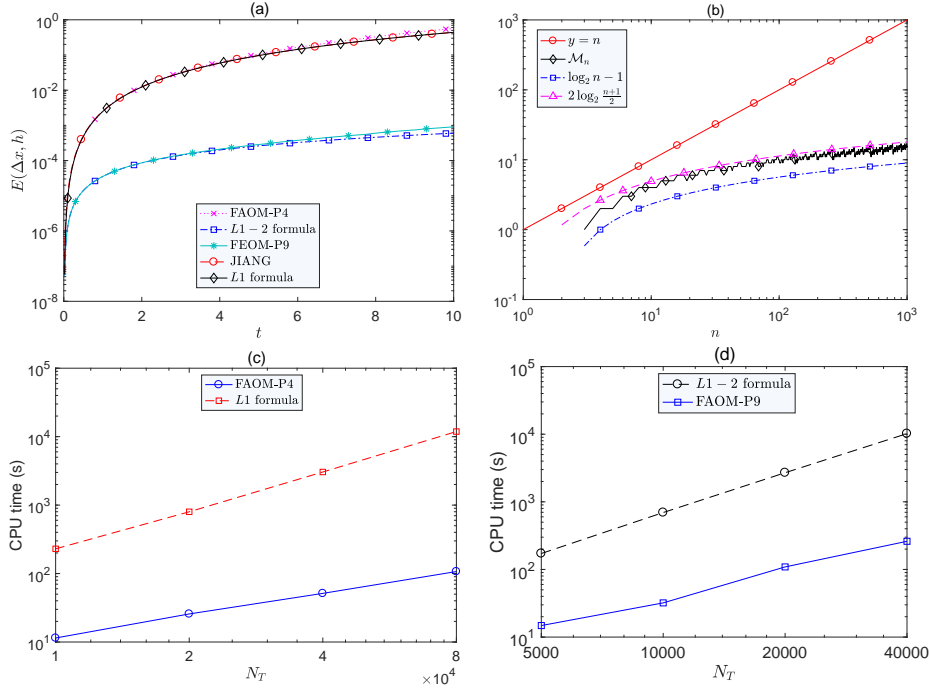


FIG. 3.2. Long time performance of the proposed methods. $\alpha = 0.5$. Here FEOM-P4 denotes the FAOM-PK method with $\Pi_{1,h}u(t)$ interpolation approximation and an approximation of $\frac{1}{(1-\tau)^\alpha}$ by a polynomial of the fourth degree. FAOM-P9 denotes the FAOM-PK method with $\Pi_{2,h}u(t)$ interpolation approximation and an approximation of $\frac{1}{(1-\tau)^\alpha}$ by a polynomial of the ninth degree. (a) The error $E(\Delta x, h)$ at each time step for the given methods are given. (b) The relationship between \mathcal{M}_n (the length of the vector $\mathbf{U}^{n,k}$) and n at each time step. (c) The total computational times for the FAOM-P4 algorithm and L1 formula with $N = 21$ and $\alpha = 0.5$. (d) The total computational times for the FAOM-P9 algorithm and L1-2 formula with $N = 21$ and $\alpha = 0.5$.

value $\varphi(x, t)$ are given by

$$\begin{aligned}
 f(u) &= 0.01u(1-u), \\
 g(x, t) &= \Gamma(4+\alpha)x^4(\pi-x)^4 \exp(-x)t^{3+\alpha}/6 - x^2(\pi-x)^2 \{t^{3+\alpha} \exp(-x) \\
 &\quad [x^2(56-16x+x^2) - 2\pi x(28-12x+x^2) + \pi^2(12-8x+x^2)] \\
 &\quad + 4(3\pi^2 - 14\pi x + 14x^2)\} - 0.01x^4(\pi-x)^4 [\exp(-x)t^{3+\alpha} + 1] \\
 &\quad \{1 - x^4(\pi-x)^4 [\exp(-x)t^{3+\alpha} + 1]\} \quad x \in \Omega_x, t \in (0, T], \\
 u_0(x) &= 0 \quad x \in \Omega_x, \\
 \varphi(x, t) &= x^4(\pi-x)^4 [\exp(-x)t^{3+\alpha} + 1] \quad x \in \partial\Omega_x, t \in (0, T].
 \end{aligned} \tag{4.3}$$

It is clear that the nonlinear problem (4.1) has the following exact solution

$$u(x, t) = x^4(\pi-x)^4 [\exp(-x)t^{3+\alpha} + 1] \quad x \in \Omega_x, t \in [0, T]. \tag{4.4}$$

We test the accuracy of the FAOM-PK algorithm for the nonlinear fractional diffusion equation with $\alpha = 0.25, 0.5$, and 0.9 . To understand the accuracy of the FAOM-PK scheme in time, we solve the problem with different time step sizes $h = 1/10, 1/20, 1/40, 1/80, 1/160$, and a fixed spatial mesh size $\Delta x = \pi/5000$. For the

reason of comparison, we also simulate the example by the direct method, i.e., the $L1$ formula and $L1 - 2$ formula. The computational errors and numerical convergence orders for the different methods with $\alpha = 0.25, 0.5$, and 0.9 are given in Table 4.1. As reported in the table, both the direct method and the FAOM-PK algorithm reach the ideal convergence orders, which are $2 - \alpha$ and $3 - \alpha$, respectively. To check the convergence rate of our FAOM-PK method in space, we simulate the case with different spatial mesh sizes $\Delta x = \pi/80, \pi/40, \pi/160, \pi/320, \pi/640$ and a fixed time step size $h = 2^{-14}$. The results are given in Table 4.2, which clearly shows that the FAOM-PK has almost the same accuracy as the corresponding direct method, but takes much less computational time.

TABLE 4.1

The errors and convergence orders in time with fixed spatial mesh size $\Delta x = \pi/5000$ for the proposed methods. $T = 1, N_\tau = 2$.

| h | $L1$ formula | | | | $L1 - 2$ formula | | | |
|-----------------|----------------------|-------|-------------------|-------|----------------------|-------|-------------------|-------|
| | <u>Direct scheme</u> | | <u>FAOM-P4</u> | | <u>Direct scheme</u> | | <u>FAOM-P9</u> | |
| | $E(\cdot, \cdot)$ | r_t | $E(\cdot, \cdot)$ | r_t | $E(\cdot, \cdot)$ | r_t | $E(\cdot, \cdot)$ | r_t |
| $\alpha = 0.9$ | | | | | | | | |
| 1/10 | 3.72e-1 | 1.25 | 3.72e-1 | 1.25 | 6.76e-2 | 2.18 | 6.76e-2 | 2.18 |
| 1/20 | 1.56e-1 | 1.19 | 1.56e-1 | 1.19 | 1.49e-2 | 2.16 | 1.49e-2 | 2.16 |
| 1/40 | 6.86e-2 | 1.15 | 6.87e-2 | 1.14 | 3.33e-3 | 2.13 | 3.33e-3 | 2.13 |
| 1/80 | 3.10e-2 | 1.12 | 3.10e-2 | 1.12 | 7.61e-4 | 2.11 | 7.61e-4 | 2.11 |
| 1/160 | 1.42e-2 | - | 1.43e-2 | - | 1.76e-4 | - | 1.77e-4 | - |
| $\alpha = 0.5$ | | | | | | | | |
| 1/10 | 1.19e-1 | 1.68 | 1.19e-2 | 1.68 | 2.06e-2 | 2.70 | 2.06e-2 | 2.70 |
| 1/20 | 3.71e-2 | 1.65 | 3.71e-2 | 1.64 | 3.17e-3 | 2.70 | 3.16e-3 | 2.69 |
| 1/40 | 1.18e-2 | 1.61 | 1.19e-2 | 1.61 | 4.91e-4 | 2.63 | 4.91e-4 | 2.63 |
| 1/80 | 3.87e-3 | 1.60 | 3.89e-3 | 1.57 | 7.94e-5 | 2.42 | 7.94e-5 | 2.41 |
| 1/160 | 1.29e-3 | - | 1.31e-3 | - | 1.48e-5 | - | 1.49e-5 | - |
| $\alpha = 0.25$ | | | | | | | | |
| 1/10 | 7.22e-2 | 1.88 | 7.22e-2 | 1.88 | 1.27e-2 | 2.91 | 1.27e-2 | 2.91 |
| 1/20 | 1.96e-2 | 1.89 | 1.96e-2 | 1.89 | 1.70e-3 | 2.90 | 1.70e-3 | 2.90 |
| 1/40 | 5.30e-3 | 1.89 | 5.31e-3 | 1.88 | 2.27e-4 | 2.82 | 2.27e-4 | 2.82 |
| 1/80 | 1.43e-3 | 1.87 | 1.44e-3 | 1.86 | 3.22e-5 | 2.28 | 3.22e-5 | 2.28 |
| 1/160 | 3.91e-4 | - | 3.97e-4 | - | 6.64e-6 | - | 6.64e-6 | - |

TABLE 4.2

The errors and convergence orders in space with fixed time step size $h = 2^{-14}$ for the proposed methods. $N_\tau = 2, T = 1, \alpha = 0.25$. Here CPU denotes the total compute time on the finest mesh.

| Δx | $L1$ formula | | | | $L1 - 2$ formula | | | |
|------------|----------------------|-------|-------------------|-------|----------------------|-------|-------------------|-------|
| | <u>Direct scheme</u> | | <u>FAOM-P4</u> | | <u>Direct scheme</u> | | <u>FAOM-P9</u> | |
| | $E(\cdot, \cdot)$ | r_s | $E(\cdot, \cdot)$ | r_s | $E(\cdot, \cdot)$ | r_s | $E(\cdot, \cdot)$ | r_s |
| $\pi/80$ | 1.12e-2 | 2.00 | 1.12e-2 | 2.00 | 1.12e-2 | 2.00 | 1.12e-2 | 2.00 |
| $\pi/160$ | 2.81e-3 | 2.00 | 2.80e-3 | 2.00 | 2.81e-3 | 2.00 | 2.80e-3 | 2.00 |
| $\pi/320$ | 7.01e-4 | 2.00 | 7.02e-4 | 1.98 | 7.01e-4 | 2.00 | 7.01e-4 | 2.00 |
| $\pi/640$ | 1.75e-4 | - | 1.78e-4 | - | 1.75e-4 | - | 1.75e-4 | - |
| CPU(s) | 807.43 | | 40.50 | | 1451.29 | | 70.85 | |

We next consider the initial value problem of the nonlinear fractional diffusion equation on the unbounded domain as follows

$$\begin{aligned} {}_0^C \mathcal{D}_t^\alpha u(x, t) &= u_{xx}(x, t) + f(u) & x \in \mathbb{R}, t > 0, \\ u(x, 0) &= u_0(x) & x \in \mathbb{R}. \end{aligned} \quad (4.5)$$

By setting $f(u) = -u(1 - u)$, (4.5) is the time fractional Fisher equation which is used in an infinite medium [5], the chemical kinetics [22], flame propagation [7], and many other scientific problems [24]. By setting $f(u) = -0.1u(1 - u)(u - 0.001)$, (4.5) is the time fractional Huxley equation, which is used to describe the transmission of nerve impulses [6, 26] with many applications in biology and the population genetics in circuit theory [31].

If the initial data $u_0(x)$ is compactly supported on $\Omega_x = [a, b]$, we solve the fractional diffusion equation (4.5) on a bounded domain $[a, b]$ with absorbing boundary conditions (ABCs) [15]. The inner points is still discretized by the first equation of (4.2) and the discretization of the points on the boundary is given by the ABCs as follows

$$\begin{aligned} (\tilde{\delta}_x + 3s_0^{\frac{\alpha}{2}})_0^C \mathcal{D}_t^{F,\alpha} u(x_{N-1}, t_{j+1}) + (3s_0^\alpha \tilde{\delta}_x + s_0^{\frac{3\alpha}{2}}) u_{N-1}^{j+1} &= (\tilde{\delta}_x + 3s_0^{\frac{\alpha}{2}}) f(\tilde{u}_{N-1}^{j+1}), \\ (\tilde{\delta}_x - 3s_0^{\frac{\alpha}{2}})_0^C \mathcal{D}_t^{F,\alpha} u(x_1, t_{j+1}) + (3s_0^\alpha \tilde{\delta}_x - s_0^{\frac{3\alpha}{2}}) u_1^{j+1} &= (\tilde{\delta}_x - 3s_0^{\frac{\alpha}{2}}) f(\tilde{u}_1^{j+1}), \end{aligned} \quad (4.6)$$

where $\tilde{\delta}_x u_i^{j+1} = \frac{u_{i+1}^{j+1} - u_{i-1}^{j+1}}{2\Delta x}$ and $s_0 = 3$ according to [15].

Example 4.2 We consider the time fractional Fisher equation with $f(u) = -u(1 - u)$ in (4.5) and initial condition

$$u(x, 0) = \sqrt{\frac{10}{\pi}} \exp(-10x^2).$$

The computational domain is set as $[-6, 6]$. Since it is difficult to obtain the exact solution of the time fractional equation on the unbounded domain, here and below we take the solution on a very fine mesh as the reference solution. Table 4.3 presents the numerical results for $\alpha = 0.25$ and 0.75 , which shows that the FAOM-PK algorithm has the same convergence order in time as the corresponding direct scheme. The convergence orders in time of the direct scheme and the FAOM-PK algorithm are higher than 1, but lower than the ideal convergence order. To understand it, we plot the numerical solution in Fig. 4.1, which shows that $u'(t)$ has singularity at $t = 0$. How to obtain a high accurate method for the solution with singularity is still an unsolved problem. Due to the approximation of $f(u)$, the convergence rate in time of our scheme is high than the scheme reported in [11, 15]. Table 4.4 indicates that the FAOM-PK algorithm has the second-order of accuracy in space and takes less computational time than the direct algorithm.

Example 4.3. We consider the time fractional Huxley equation with $f(u) = -0.1u(1 - u)(u - 0.001)$ in (4.5) and initial condition

$$u(x, 0) = \exp(-10(x - 0.5)^2) + \exp(-10(x + 0.5)^2).$$

The computational domain is set as $[-8, 8]$. Table 4.5 presents the numerical results for $\alpha = 0.5$, which shows that the FAOM-PK algorithm has the same convergence order in time as the corresponding direct scheme. Similar to the above example, the convergence orders in time of the direct scheme and the FAOM-PK algorithm are

TABLE 4.3

The errors and convergence orders for the Fisher equation in time with fixed spatial mesh size $\Delta x = 3 \times 2^{-10}$ for the proposed methods. $N_\tau = 2$, $T = 1$.

| h | $L1$ formula | | | | $L1 - 2$ formula | | | |
|-----------------|-------------------------|-------|-------------------------|-------|-------------------------|-------|-------------------------|-------|
| | Direct scheme | | FAOM-P4 | | Direct scheme | | FAOM-P9 | |
| | $\ e^{N_\tau}\ _\infty$ | r_t | $\ e^{N_\tau}\ _\infty$ | r_t | $\ e^{N_\tau}\ _\infty$ | r_t | $\ e^{N_\tau}\ _\infty$ | r_t |
| $\alpha = 0.25$ | | | | | | | | |
| 2^{-8} | 1.92e-4 | 1.15 | 1.93e-4 | 1.14 | 1.81e-4 | 1.16 | 1.88e-4 | 1.15 |
| 2^{-9} | 8.63e-5 | 1.27 | 8.74e-5 | 1.24 | 8.12e-5 | 1.28 | 8.49e-5 | 1.26 |
| 2^{-10} | 3.57e-5 | 1.63 | 3.70e-5 | 1.52 | 3.35e-5 | 1.63 | 3.54e-5 | 1.59 |
| 2^{-11} | 1.16e-5 | - | 1.29e-5 | - | 1.08e-5 | - | 1.17e-5 | - |
| $\alpha = 0.75$ | | | | | | | | |
| 2^{-8} | 3.19e-4 | 1.21 | 3.18e-4 | 1.21 | 2.27e-4 | 1.36 | 2.36e-4 | 1.34 |
| 2^{-9} | 1.38e-4 | 1.29 | 1.37e-4 | 1.30 | 8.85e-5 | 1.44 | 9.34e-5 | 1.41 |
| 2^{-10} | 5.65e-5 | 1.62 | 5.58e-5 | 1.66 | 3.26e-5 | 1.75 | 3.52e-5 | 1.68 |
| 2^{-11} | 1.83e-5 | - | 1.76e-5 | - | 9.67e-6 | - | 1.10e-5 | - |

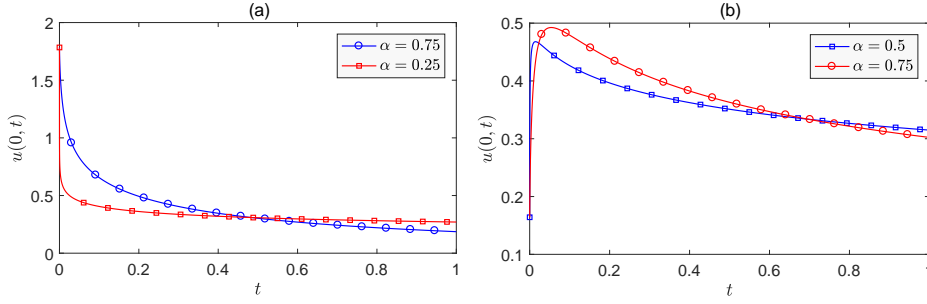


FIG. 4.1. Numerical solutions at $x = 0$. (a) The time fractional Fisher equation with $\alpha = 0.25, 0.75$. (b) The time fractional Huxley equation with $\alpha = 0.5, 0.75$.

higher than 1, but lower than the ideal convergence order. Due to the approximation of $f(u)$, the convergence order in time of our scheme is higher than the scheme reported in [11, 15]. Table 4.6 indicates that the FAOM-PK algorithm has the second-order of accuracy in space and takes less computational time than the direct algorithm.

5. Conclusions. In this paper, we present a high order fast algorithm with almost optimum memory for the Caputo fractional derivative. The fast algorithm is based on a nonuniform split of the interval $[0, t_n]$ and a polynomial approximation of the kernel function $(1 - \tau)^{-\alpha}$, in which the storage requirement and computational cost both are reduced from $O(n)$ to $O(\log n)$. We prove that the fast algorithm has the same convergence rate as that of the corresponding direct method, even a high order scheme is compared. The fast algorithm is applied to solve the linear and nonlinear fractional diffusion equations. Numerical results on linear and nonlinear fractional diffusion equations show that our fast scheme has the same order of convergence as the corresponding direct methods, but takes much less computational time.

REFERENCES

TABLE 4.4

The errors and convergence orders for the Fisher equation in space with fixed time step size $h = 2^{-14}$ for the proposed methods. $N_\tau = 2$, $T = 1$. Here CPU denotes the total compute time on the finest mesh.

| Δx | Direct scheme | | FAOM-P4 | | Direct scheme | | FAOM-P4 | |
|------------|-------------------------------|-------|-------------------------------|-------|-------------------------------|-------|-------------------------------|-------|
| | $\ \mathbf{e}^{N_T}\ _\infty$ | r_s | $\ \mathbf{e}^{N_T}\ _\infty$ | r_s | $\ \mathbf{e}^{N_T}\ _\infty$ | r_s | $\ \mathbf{e}^{N_T}\ _\infty$ | r_s |
| | $\alpha = 0.25$ | | | | $\alpha = 0.75$ | | | |
| $3/2^5$ | 6.92e-4 | 2.03 | 6.94e-4 | 2.02 | 3.53e-4 | 2.03 | 3.53e-4 | 2.04 |
| $3/2^6$ | 1.69e-4 | 2.07 | 1.71e-4 | 2.04 | 8.66e-5 | 2.07 | 8.58e-5 | 2.12 |
| $3/2^7$ | 4.03e-5 | 2.32 | 4.17e-5 | 2.14 | 2.06e-5 | 2.32 | 1.98e-5 | 2.60 |
| $3/2^8$ | 8.05e-6 | - | 9.48e-6 | - | 4.12e-6 | - | 3.34e-6 | - |
| CPU(s) | 938.50 | | 33.46 | | 905.82 | | 29.15 | |

TABLE 4.5

The errors and convergence orders for the Huxley equation in time with fixed spatial mesh size $\Delta x = 2^{-6}$ for the proposed methods. $N_\tau = 2$, $T = 1$, $\alpha = 0.5$.

| h | L1 formula | | | | L1 - 2 formula | | | |
|----------|-------------------------------|-------|-------------------------------|-------|-------------------------------|-------|-------------------------------|-------|
| | Direct scheme | | FAOM-P4 | | Direct scheme | | FAOM-P9 | |
| | $\ \mathbf{e}^{N_T}\ _\infty$ | r_t | $\ \mathbf{e}^{N_T}\ _\infty$ | r_t | $\ \mathbf{e}^{N_T}\ _\infty$ | r_t | $\ \mathbf{e}^{N_T}\ _\infty$ | r_t |
| 2^{-5} | 8.94e-4 | 1.13 | 8.94e-4 | 1.12 | 5.49e-4 | 1.10 | 6.29e-4 | 1.10 |
| 2^{-6} | 4.10e-4 | 1.24 | 4.10e-4 | 1.24 | 2.56e-4 | 1.23 | 2.94e-4 | 1.21 |
| 2^{-7} | 1.73e-4 | 1.60 | 1.74e-4 | 1.58 | 1.09e-4 | 1.60 | 1.28e-4 | 1.50 |
| 2^{-8} | 5.72e-5 | - | 5.81e-5 | - | 3.59e-5 | - | 4.51e-5 | - |

- [1] D. BAFFET AND J. S. HESTHAVEN, *A kernel compression scheme for fractional differential equations*, SIAM J. Numer. Anal., 55(2) (2017), pp. 496–520.
- [2] J. CAO AND C. XU, *A high order scheme for the numerical solution of the fractional ordinary differential equations*, J. Comput. Phys., 238 (2013), pp. 154–168.
- [3] C. CHEN, F. LIU, I. TURNER, AND V. ANH, *A Fourier method for the fractional diffusion equation describing sub-diffusion*, J. Comput. Phys., 227 (2007), pp. 886–897.
- [4] M. CUI, *Compact finite difference method for the fractional diffusion equation*, J. Comput. Phys., 228 (2009), pp. 7792–7804.
- [5] R. A. FISHER, *The wave of advance of advantageous genes*, Ann. Eugene, 7 (1937), pp. 335–369.
- [6] R. FITZHUGH, *Impulse and physiological states in models of nerve membrane*, Biophys. J., 1 (1961), pp. 445–466.
- [7] D. A. FRANK, *Diffusion and heat exchange in chemical kinetics*, Princeton University Press, Princeton, NJ, USA.
- [8] G. H. GAO, Z. Z. SUN AND H. W. ZHANG, *A new fractional numerical differentiation formula to approximate the Caputo fractional derivative and its applications*, J. Comput. Phys., 259 (2014), pp. 33–50.
- [9] G. H. GAO, Z. Z. SUN, AND Y. N. ZHANG, *A finite difference scheme for fractional sub-diffusion equations on an unbounded domain using artificial boundary conditions*, J. Comput. Phys., 231 (2012), pp. 2865–2879.
- [10] G. H. GAO AND Z. Z. SUN, *The finite difference approximation for a class of fractional sub-diffusion equations on a space unbounded domain*, J. Comput. Phys., 236 (2013), pp. 443–460.
- [11] S. D. JIANG, J. W. ZHANG, Q. ZHANG, AND Z. M. ZHANG, *Fast evaluation of the Caputo fractional derivative and its applications to fractional diffusion equations*, Commun. Comput. Phys., 21(3) (2017), pp. 650–678.
- [12] A. KILBAS, H. SRIVASTAVA, AND J. TRUJILLO, *Theory and Applications of Fractional Differential Equations*, Elsevier Science and Technology, Boston, 2006.
- [13] T. LANGLANDS AND B. HENRY, *The accuracy and stability of an implicit solution method for the fractional diffusion equation*, J. Comput. Phys., 205 (2005), pp. 719–736.
- [14] T. LANGLANDS AND B. HENRY, *Fractional chemotaxis diffusion equations*, Phys. Rev. E, 81 (2010), pp. 051102.

TABLE 4.6

The errors and convergence orders for the Huxley equation in space with fixed time step size $h = 2^{-14}$ for the proposed methods. $N_\tau = 2$, $T = 1$. Here CPU denotes the total compute time on the finest mesh.

| Δx | Direct scheme | | FAOM-P4 | | Direct scheme | | FAOM-P4 | |
|------------|----------------------------------|-------|----------------------------------|-------|----------------------------------|-------|----------------------------------|-------|
| | $\ \mathbf{e}^{N_\tau}\ _\infty$ | r_s | $\ \mathbf{e}^{N_\tau}\ _\infty$ | r_s | $\ \mathbf{e}^{N_\tau}\ _\infty$ | r_s | $\ \mathbf{e}^{N_\tau}\ _\infty$ | r_s |
| | $\alpha = 0.5$ | | | | $\alpha = 0.75$ | | | |
| 2^{-2} | 2.14e-3 | 2.14 | 2.14e-3 | 2.13 | 1.41e-3 | 2.12 | 1.41e-3 | 2.12 |
| 2^{-3} | 4.88e-4 | 2.10 | 4.89e-4 | 2.08 | 3.24e-4 | 2.09 | 3.24e-4 | 2.10 |
| 2^{-4} | 1.14e-4 | 2.33 | 1.15e-4 | 2.27 | 7.61e-5 | 2.33 | 7.57e-5 | 2.36 |
| 2^{-5} | 2.27e-5 | - | 2.40e-5 | - | 1.52e-5 | - | 1.47e-5 | - |
| CPU(s) | 743.33 | | 25.81 | | 773.61 | | 25.73 | |

- [15] D. F. LI AND J. W. ZHANG, *Efficient implementation to numerically solve the nonlinear time fractional parabolic problems on unbounded spatial domain*, J. Comput. Phys., 322 (2016), pp. 415–428.
- [16] J. R. LI, *A fast time stepping method for evaluating fractional integrals*, SIAM J. Sci. Comput., 31(6) (2010), pp. 4696–4714.
- [17] X. LI AND C. XU, *A Space-time spectral method for the time fractional diffusion equation*, SIAM J. Numer. Anal., 47 (2009), pp. 2108–2131.
- [18] Y. LIN, X. LI, AND C. XU, *Finite difference/spectral approximations for the fractional cable equation*, Math. Comp. 80 (2011), pp. 1369–1396.
- [19] Y. LIN AND C. XU, *Finite difference/spectral approximations for the time-fractional diffusion equation*, J. Comput. Phys., 225 (2007) pp. 1533–1552.
- [20] M. LÓPEZ-FERNÁNDEZ, C. LUBICH, AND A. SCHÄDLE, *Adaptive, fast, and oblivious convolution in evolution equations with memory*, SIAM J. Sci. Comput., 30(2) (2008), pp. 1015–1037.
- [21] C. LUBICH AND A. SCHÄDLE, *Fast convolution for nonreflecting boundary conditions*, SIAM J. Sci. Comput., 24(1) (2002), pp. 161–182.
- [22] W. MALFLICT, *Solitary wave solutions of nonlinear wave equations*, Am. J. Phys., 60 (1992), pp. 650–654.
- [23] W. MCLEAN, *Fast summation by interval clustering for an evolution equation with memory*, SIAM J. Sci. Comput., 34(6) (2012), pp. A3039–A3056.
- [24] M. MERDAN, *Solutions of time-fractional reaction-diffusion equation with modified Riemann–Liouville derivative*, Int. J. Phys. Sci., 7 (2012), pp. 2317–2326.
- [25] R. METZLER AND J. KLAFTER, *The random walks guide to anomalous diffusion: a fractional dynamics approach*, Phys. Rep., 339 (2000), pp. 1–77.
- [26] J. S. NAGUMO, S. ARIMOTO, AND S. YOSHIZAWA, *An active pulse transmission line simulating nerve axon*, Proc. IRE, 50 (1962), pp. 2061–2070.
- [27] K. B. OLDHAM AND J. SPANIER, *The Fractional Calculus*, Academic Press, New York, 1974.
- [28] I. PODLUBNY, *Fractional Differential Equations*, Academic Press, New York, 1999.
- [29] J. REN, Z. SUN, AND W. DAI, *New approximations for solving the Caputo-type fractional partial differential equations*, Appl. Math. Model., 40 (2016), pp. 2625–2636.
- [30] A. SCHÄDLE, M. LÓPEZ-FERNÁNDEZ, AND C. LUBICH, *Fast and oblivious convolution quadrature*, SIAM J. Sci. Comput., 28(2) (2006), pp. 421–438.
- [31] M. SHIH, E. MOMONIAT, AND F. M. MAHOMED, *Approximate conditional symmetries and approximate solutions of the perturbed Fitzhugh–Nagumo equation*, J. Math. Phys., 46 (2005), pp. 023503.
- [32] Z. SUN AND X. WU, *A fully discrete difference scheme for a diffusion-wave system*, Appl. Numer. Math., 56 (2006), pp. 193–209.
- [33] Q. YANG, I. TURNER, F. LIU, AND M. ILIS, *Novel numerical methods for solving the time-space fractional diffusion equation in 2D*, SIAM J. Sci. Comput., 33 (2011), pp. 1159–1180.
- [34] F. ZENG, C. LI, F. LIU, AND I. TURNER, *Numerical algorithms for time-fractional subdiffusion equation with second-order accuracy*, SIAM J. Sci. Comput., 37 (2015), pp. A55–A78.
- [35] F. ZENG, I. TURNER, AND K. BURRAGE, *A stable fast time-stepping method for fractional integral and derivative operators*, arXiv:1703.05480, 2017.
- [36] Y. N. ZHANG, Z. Z. SUN, AND H. W. WU, *Error estimates of Crank–Nicolson-type difference scheme for the subdiffusion equation*, SIAM J. Numer. Anal., 49 (2011), pp. 2302–2322.